PREPARATION, SPECTRAL CHARACTERIZATION, MOLECULAR DOCKING, AND ANTIOXIDANT ACTIVITY OF NEW SYMMETRICAL DIMERS DERIVATIVES OF OXAZEPINE STARTING FROM PYRIDINE-5,7-DIONE ANHYDRIDE

Rasim F. Muslim[1], Ahmed F. Shallal[2], Manaf A. Guma[3*], Noor S. Ibrahim[4]

[1]Department of Applied Chemistry, College of Applied Sciences-Hit, University of Anbar, Anbar, Iraq.
[2]Department of Biology, College of Science, University of Raparin, Rania, Sulaymaneyah Governorate 46012
[3]Department of Environment, College of Applied Sciences-Hit, University of Anbar, Anbar, Iraq.
[4]University Headquarter, University of Anbar, Anbar, Iraq.
[*]e-mail: manafguma@uoanbar.edu.iq

Received 13.05.2025
Accepted 29.08.2025

Abstract: *This study reports the synthesis of a series of oxazepine derivatives via a condensation reaction between amines and various benzaldehyde derivatives, using benzene as the solvent. The resulting intermediates were subsequently reacted with pyridine-5,7-dione anhydride in dry benzene to afford oxazepine derivatives (H_1–H_6). The synthesized compounds were characterized by Fourier-transform infrared (FT-IR) spectroscopy, proton nuclear magnetic resonance (^{1}H-NMR) spectroscopy, and mass spectrometry. Reaction progress was monitored using thin-layer chromatography (TLC).*
The antioxidant activity of compounds H_1–H_6 was evaluated and compared with that of vitamin C. In addition, molecular docking studies were performed for selected compounds (H_1, H_4, and H_6) against tyrosinase (PDB ID: 3NM8) to identify optimal binding sites and evaluate interactions with neighboring residues. The docked complexes exhibited RMSD values of 1.16, 1.40, and 1.30 Å for H_1, H_4, and H_6, respectively. Among the tested compounds, H_4 showed the highest binding affinity, in good agreement with the experimental results.
Overall, the synthesized oxazepine derivatives demonstrated moderate antioxidant activity, warranting further in vivo investigation.
Keywords*: Pyridine-5,7-dione anhydride, Antioxidant activity, Oxazepine derivatives, docked protein.*

1. Introduction

Oxazepine derivatives represent a great class of heterocyclic compounds that can be illustrated by a seven-membered ring involving both nitrogen and oxygen atoms [1–4]. The particular chemical structures with unique functional groups of oxazepine have been established to develop new biologically active molecules (Fig. 1). Structural modifications of the oxazepine that can involve a lactam ring with other sulfur substituents fused within oxazepine rings have exhibited more biologically active compounds [5–8].

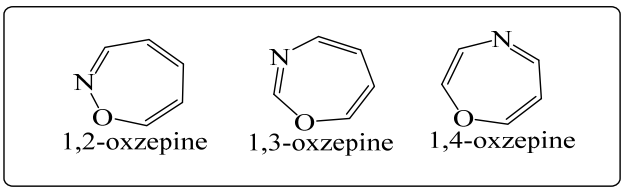

Fig. 1. Oxazepine derivatives

Oxazepine derivatives exhibit stability due to conjugation between the double bonds within the ring structure. Some oxazepine derivatives were previously prepared through the Schiff base reaction with cyclic anhydrides. Oxazepine derivatives have garnered significant attention from researchers due to their biological activity against various viruses, bacteria, fungi, and cancerous tumors [5, 9, 10]. They have also demonstrated pharmaceutical potential, including antimicrobial, anticonvulsant, anxiolytic, and analgesic activities [11, 12].

Recent studies have reported innovative techniques for the synthesis and functionalization of oxazepine derivatives. For example, about five compounds have been recently reported involving bicyclic δ–lactam–oxazepine compounds containing a sulfur substituent prepared using an economical synthetic route, showing remarkable biological activity as an antibacterial agent [13]. Another current study reported the preparation, spectral characterization, in silico ADME profiling, molecular docking, and antioxidant activity of multiple symmetrical dimeric oxazepine derivatives, showing insights into their pharmacokinetic features and antioxidant activity [14].

Schiff bases serve as a fundamental material in the synthesis of numerous organic, biological, and industrial compounds [15, 16].

Including non-homogeneous cyclic compounds through ring-closure reactions, ring addition, and substitution reactions [17, 18]. Schiff bases were first synthesized by the German scientist Hugo Schiff in 1864 [19], through the condensation of a carbonyl group with an aldehyde or a ketone with a primary amine [18]. They were renamed as imine or azomethine compounds [19–22].

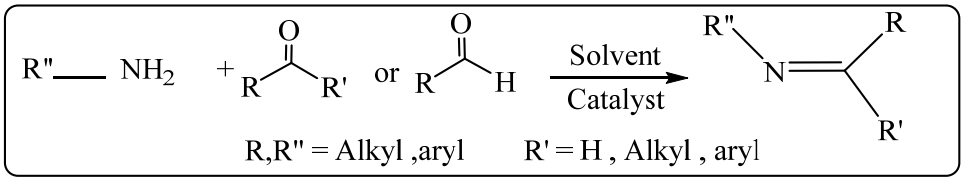

Scheme 1. Proposed mechanism for the formation of Azomethine compounds

The general structural formula of Schiff bases is (R"N=CR'R), where (R", R', R) can be aryl, alkyl, hydrogen, or non-homogeneous rings [26–23]. Schiff bases receive alternative names due to variations in the groups (R", R', R) attached to the carbon and nitrogen atoms forming the (C=N) bond [25]. They are called benzoylates when prepared from aniline and benzaldehyde exclusively [23], as well as anilities when derived from anilines and their derivatives [27]. They are also known as ketimines when synthesized from ketones and amines and aldimines when prepared from aldehydes and amines [28]. Schiff bases have two geometric isomers depending on the type of groups attached to the nitrogen and carbon atoms, denoted by the symbols (Z, E), derived from the German words "Entgegen", meaning opposite sides and "Zusammen", meaning same side (Figure 2) [19].

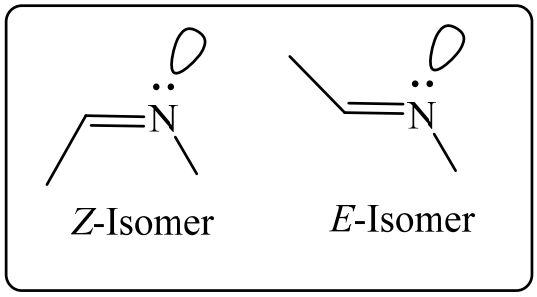

Fig. 2. Geometric isomers of azomethine compounds

The extensive biological activities of oxazepine derivatives, which have demonstrated valuable applications in the medical field, have attracted considerable research interest toward understanding their mechanisms of action. These mechanisms can be explored through advanced computational chemistry approaches, including molecular docking studies, as well as through the systematic substitution of functional groups to elucidate the influence of structural modifications on binding affinity and bioavailability, thereby facilitating rational drug design. Schiff base reactions provide an effective synthetic route for the preparation of such compounds. In this study, we aimed to synthesize new oxazepine derivatives from pyridine-5,7-dione anhydride via Schiff bases and to investigate selected biological activities.

2. Experimental part

2.1. The chemicals and solvents. All compounds of 4,4'-methylenedianiline, 1,2,4-triazole-3,5-diamine, pyridine-2,6-diamine, 4-nitrobenzaldehyde, 2,4-chlorobenzaldehyde, 4-chlorobenzaldehyde, 4-aminophenol, terephthalaldehyde, pyridine-5,7-dione anhydride, and 2,2-diphenyl-1-picrylhydrazyl (DPPH) (99%) from Sigma Aldrich Company. Absolute ethanol (99.9%) from Scharlau Company. Benzene (99.9%) from Merck Company.

2.2. General procedure for Synthesis of 7,8-dihydropyrido [1,3] oxazepine-5,9-dione [H_1-H_6]. The work method was adopted following references with some modifications [29, 30]. A quantity of 0.01 mole (1.5 gm) of 4-nitrobenzaldehyde was dissolved in 30 ml of dry benzene at the same time. A quantity of 0.005 mole (1 gm) of 4,4'-methylenedianiline was dissolved in 20 ml of the same solvent, the two solutions were mixed, the mixture was allowed to react, and the progress of the reaction was monitored by thin-layer chromatography (TLC) using the solvent mixture (methanol: cyclohexane)in a ratio of (2:7) [31].

Once the reaction of azomethine was finished, the product was then confirmed using TLC. For oxazepine synthesis, 0.01 mole (1.49 g) of pyridine-5,7-dione anhydride was added to the last product and then refluxed till the product's color changed. Once the reaction was finished, the products were confirmed using TLC using the solvent mixture (benzene:acetone) with a ratio of 6:2. The formed precipitate was collected, and it was recrystallized using absolute ethanol to obtain the H_1 compound. The remaining derivatives of 7,8-dihydropyrido [1,3] oxazepine-5,9-dione [H_2-H_6] were prepared using the same method [29, 32].

Table 1. Properties of the prepared 7,8-dihydropyrido [1,3] oxazepine-5,9-dione [H_1-H_6]

No.	Structure and nomenclature	Molecular formula	Yield%	R*f*
H_1	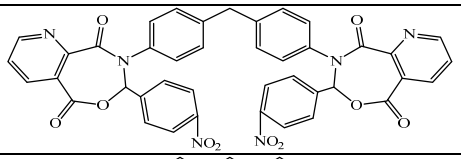	$C_{41}H_{26}N_6O_{10}$	75	0.71
H_2	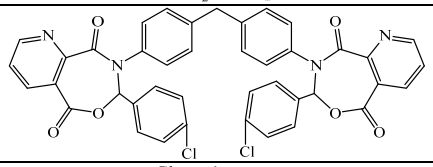	$C_{41}H_{26}Cl_2N_4O_6$	71	0.62
H_3	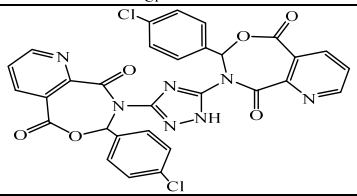	$C_{30}H_{17}Cl_2N_7O_6$	42	0.59
H_4	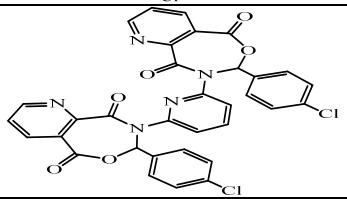	$C_{33}H_{19}Cl_2N_5O_6$	59	0.73
H_5	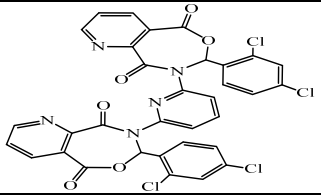	$C_{33}H_{17}Cl_4N_5O_6$	61	0.71
H_6	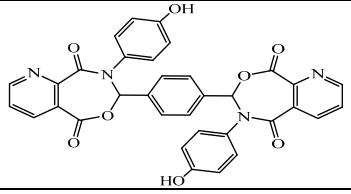	$C_{34}H_{22}N_4O_8$	57	0.64

2.3. Antioxidant activity

2.3.1. DPPH Free radical scavenging activity. The compounds were subjected to in vitro antioxidant activity testing using 2,2-diphenyl-1-picrylhydrazyl (DPPH), a method that assesses the compounds' ability to scavenge free radicals. Different concentrations were prepared by dissolving 4 mg of ascorbic acid in 100 ml of methanol to create a standard solution of 400 µg/ml. Using the standard solution, various concentrations of ascorbic acid (0.5, 0.2, 0.15, 0.1, and 0.05 mM) were prepared and utilized as the typical solution. Sample solutions were prepared by dissolving 1 mg of each sample in 1 ml of dimethyl sulfoxide (DMSO), and following the principles of molarity and dilution laws, the concentrations mentioned above were prepared. Furthermore, 4 mg of 2,2-Diphenyl-1-Picrylhydrazyl was dissolved in 100 mL of the methanol solvent; the solution was shielded from light [33, 34] [14].

2.3.2. The procedure for valuation of 2,2-Diphenyl-1-Picrylhydrazyl hunting action. The absorption of the 2,2-Diphenyl-1-Picrylhydrazyl reagent was directly measured at 517 nm for the control reading. Upon completion of meditation synthesis, 1.5 mL of the reagent was added to each test tube holding the sample and meditations of the standard solution separately. The samples were gestated in the shadowy for 30 minutes. Subsequently, the absorption was measured at 517 nm using a UV-visible spectrometer after 30 minutes, with methanol serving as the blank solution. The free radical antiradical action % was calculated by:

Antiradical activity% = (A Control - A Test) / A Control * 100
A Control = absorbance of the control reaction (containing all reagents except the sample extract) A Test = absorbance of the sample (oxazepine derivatives).

2.4. Docking of the Synthesized Novel Homo-Oxazepine Dimer Derivatives (H_1, H_4, and H_6) with the 3NM8 Reductase. The H_1, H_4 and H_6 structures were generated using ChemDraw software 2013 and then converted to SDF and MOL formats for docking purposes. The PDB of the 3NM8 of tyrosinase was retrieved from the Protein Data Bank (www.rcsb.org) [33]. The MOE Molecular Operating Environment software was used to perform the molecular docking process [35], the PLIP website was used for analysis, and PyMol software was used for visualization [33, 34, 36].

3. Results and discussion

The chemical synthesis of the new oxazepine derivatives compounds (H_1-H_6). The compounds of 7,8-dihydropyrido[1,3]oxazepine-5,9-dione derivatives were obtained by reaction between Schiff's bases and pyridine-5,7-dione anhydride [19]. All the steps of the intermediate in the reaction were confirmed using TLC. The general mechanism of the oxazepine derivatives (H_1-H_6) reactions was suggested as seen in Scheme (2).

3.1. FT-IR spectra of 7,8-dihydropyrido[1,3]oxazepine-5,9-dione derivatives (H_1-H_6). All 7,8-dihydropyrido[1,3]oxazepine-5,9-dione derivatives were confirmed using infrared spectroscopy, where all spectra showed the disappearance of the absorption band of the C=N groups of the Schiff's bases and the appearance of the lactamic (ν N-C=O) groups in the range (1655-1661 cm^{-1}) and the lactonic (ν O-C=O) groups in the range (1685-1693 cm^{-1}) (Fig.s 3-8) [37–39].

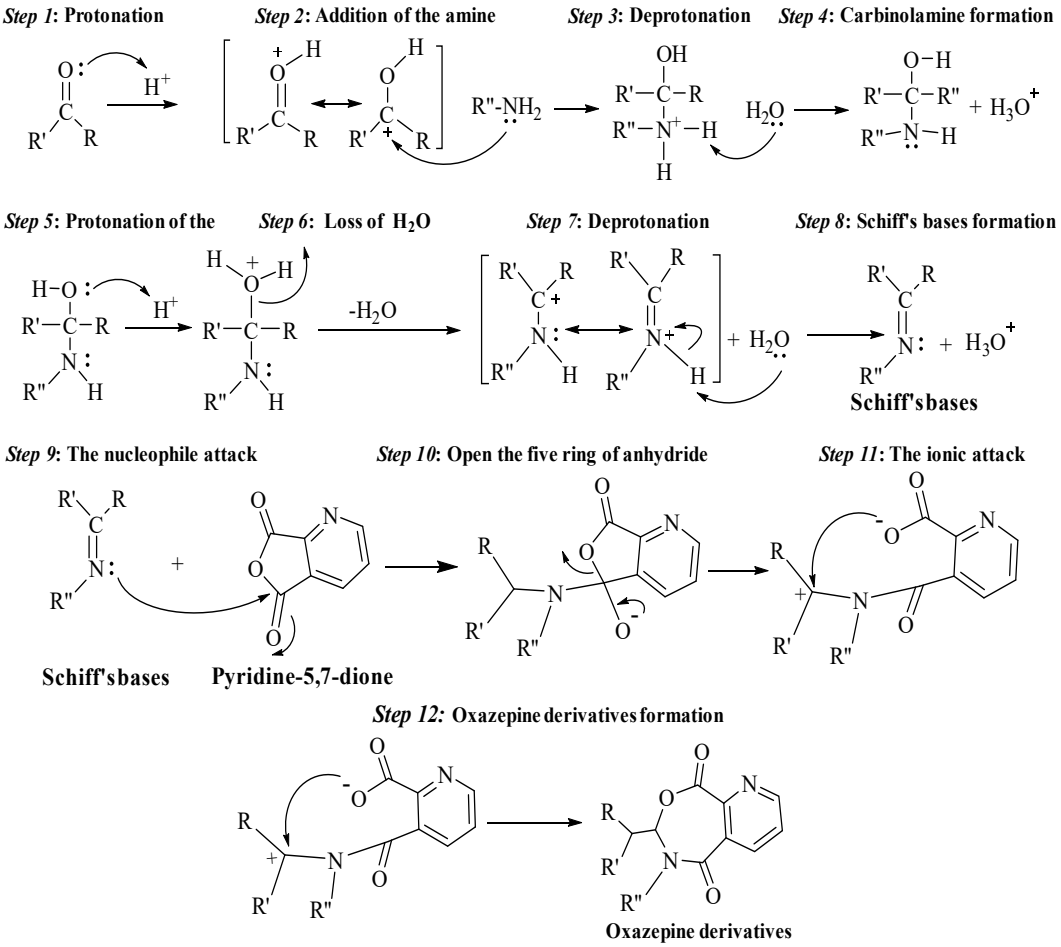

Scheme 2. The general mechanism for the preparation of the oxazepine derivatives [19]

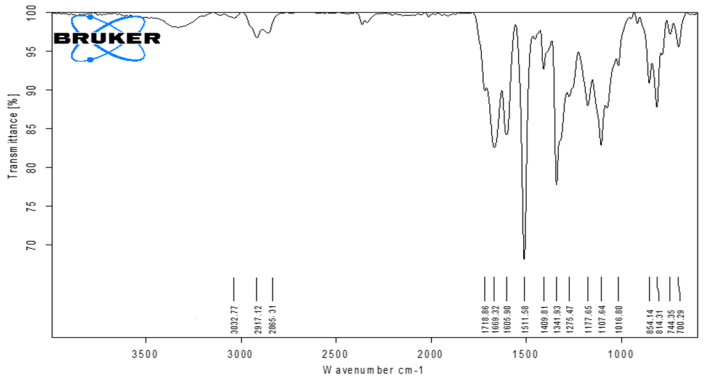

Fig. 3. FT-IR spectrum for H_1compound

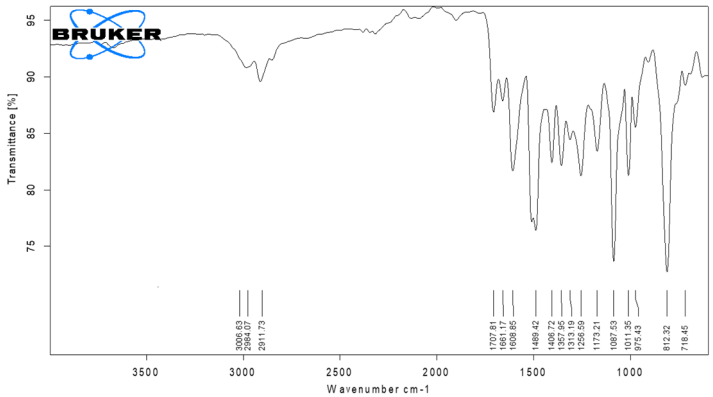

Fig. 4. FT-IR spectrum for H_2 compound

The spectra also showed other absorption bands belonging to the aggregates. Compensation in the synthesis of oxazepine derivatives and aromatic rings was followed in the FT-IR spectra in each step of the reaction [40, 41]. Table 2 shows the values of absorption bands for derivatives 7, 8-dihydropyridine[1,3] oxazepine-5,9-dione (H_1-H_6) compounds.

Table 2. The FT-IR (cm^{-1}) absorption bands of 7,8-dihydropyrido[1,3]oxazepine-5,9-dione (H_1-H_6) derivatives (Fig.s 3-8)

No	C-H Aromatic	C=C Aromatic	ν C-H Aliphtic		C=O lactone	C=O lactam	Other
			Asymmetric	Symmetric			
H_1	3032	1605	2917	2865	1718	1669	NO_2 1341 and 1511 C-N 1341 C-O 1409
H_2	3006	1608	2984	2911	1707	1661	C-Cl 1011 C-N 1357 C-O 1406
H_3	3085	1571	2920	2871	1718	1643	C-Cl 1012 C-N 1342 C-O 1407 N-H 3248 b
H_4	3059	1587	2913	2862	1714	1660	C-Cl 1014 C-N 1358 C-O 1486
H_5	3057	1583	2921	2852	1729	1654	C-Cl 1010 C-N 1357 C-O 1441
H_6	3037	1593	2923	2874	1729	1676	OH 3368 b C-N 1300 C-O 1413

b= broad

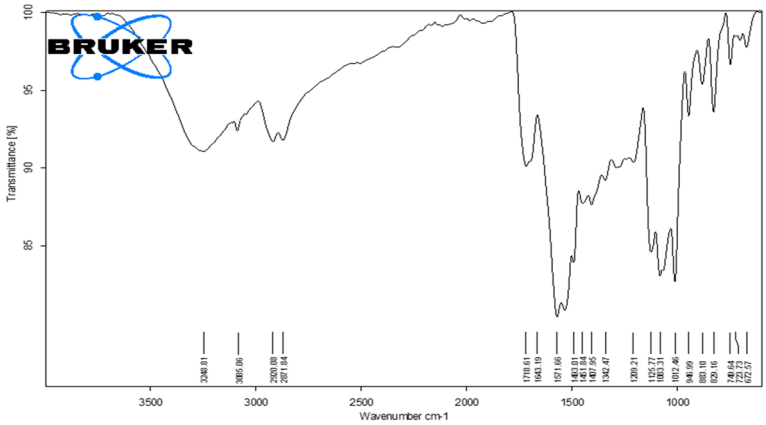

Fig. 5. FT-IR spectrum for H_3 compound

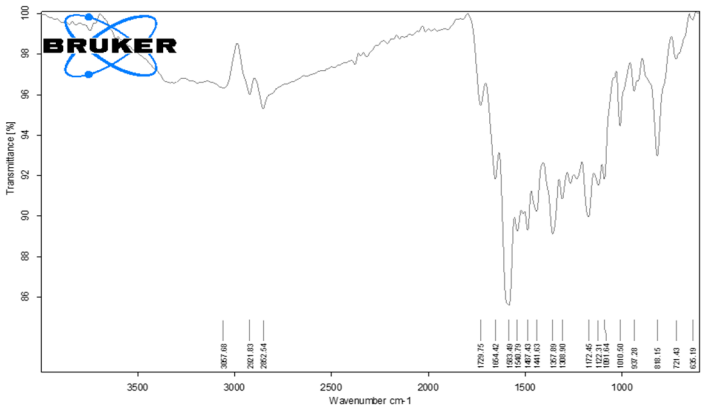

Fig. 6. FT-IR spectrum for H_4 compound

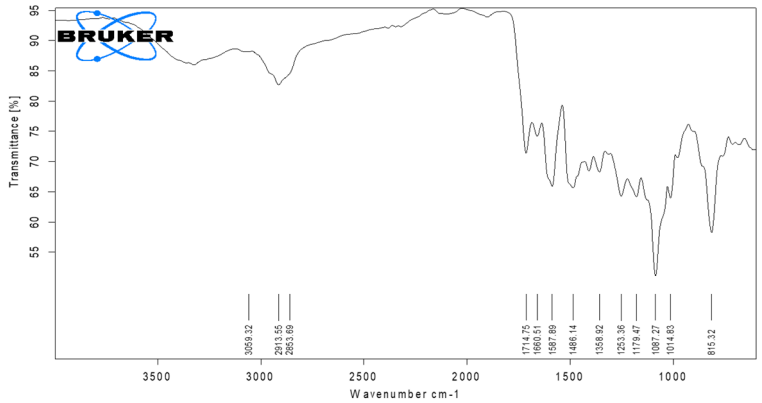

Fig. 7. FT-IR spectrum for H_5 compound

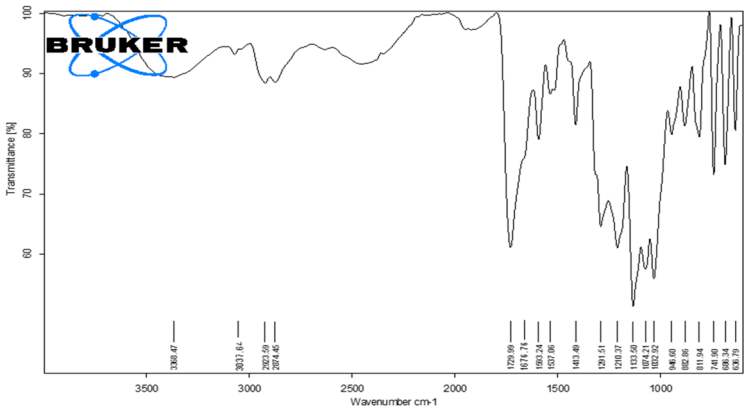

Fig. 8. FT-IR spectrum for H_6 compound

3.2. ^{1}H-NMR spectra. In all Fig. s 9–14, corresponding to the ^{1}H-NMR spectra of the 7,8-dihydropyrido[1,3]oxazepine-5,9-dione derivatives, three additional signals were observed. The first signal, appearing at 0 ppm, corresponds to the reference compound tetramethylsilane (TMS). The second signal, observed at 2.51 ppm, is attributed to the solvent dimethyl sulfoxide (DMSO) used to dissolve the samples. The third signal, appearing at approximately 3.50 ppm, arises from residual water commonly present in DMSO [42,43]. All remaining signals were in full agreement with the expected structures of the synthesized products. The assignments of the observed signals for all prepared compounds are summarized in Table 3.

Table 3. ^{1}H-NMR chemical shift values for selected 7,8-dihydropyrido [1,3] oxazepine-5,9-dione [H_1-H_6]

No	Structure	Number of protons	Type of single	Group	δ Value ppm
H_1		2	s	Ar-CH_2-Ar	4.04
		8	d d	Aromatic protons [A]	6.95-7.79
		8	d d	Aromatic protons [B]	8.17-8.41
		6	m	Pyridine protons [C]	8.76-8.89
		2	s	-N-CH-O heterocycle	9.10
H_2		2	s	Ar-CH_2-Ar	4.03
		8	d d	Aromatic protons [A]	6.77-7.39
		8	d d	Aromatic protons [B]	8.46-8.03
		6	m	Pyridine protons [C]	8.17-8.71
		2	s	-N-CH-O heterocycle	9.08
H_3		8	d d	Aromatic protons [A]	7.43-7.96
		6	m	Pyridine protons [B]	8.14-8.80
		2	s	-N-CH-O heterocycle	9.08
		1	s	NH of the cycle [C]	10.61

H_4		8	d d	Aromatic protons [A]	7.40-7.96
		3	m	Pyridine protons [B]	8.16-8.28
		6	m	Pyridine protons [C]	8.40-8.79
		2	s	-N-CH-O heterocycle	9.08
H_5		8	m	Aromatic protons [A]	7.41-7.61
		3	m	Pyridine protons [B]	7.67-8.01
		6	m	Pyridine protons [C]	8.26-8.78
		2	s	-N-CH-O heterocycle	9.08
H_6		4	d d	Aromatic protons [A]	7.11-7.18
		8	d d	Aromatic protons [B]	7.51-7.66
		6	m	Pyridine protons [C]	8.79-8.80
		2	s	-N-CH-O heterocycle	9.08
		2	s	-OH	9.66

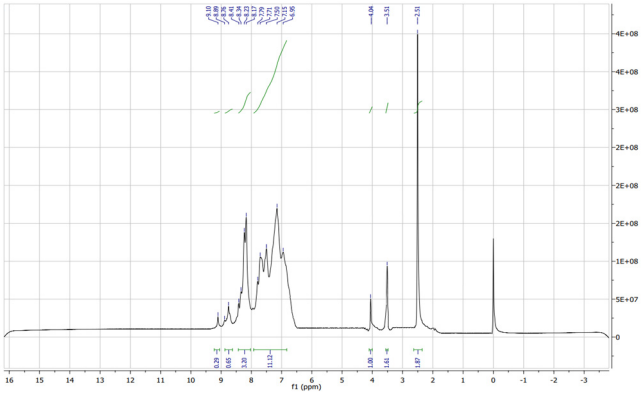

Fig. 9. ^{1}H-NMR spectrum for H_1 compound

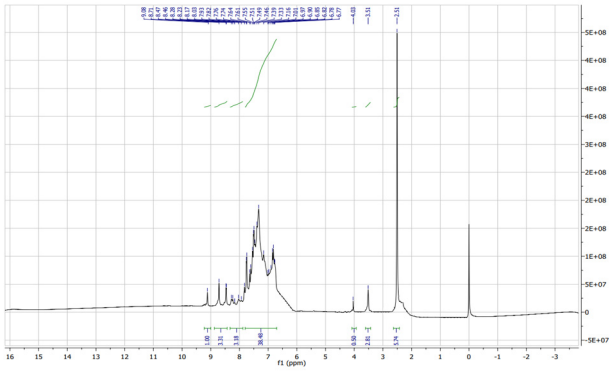

Fig. 10. ^{1}H-NMR spectrum for H_2 compound

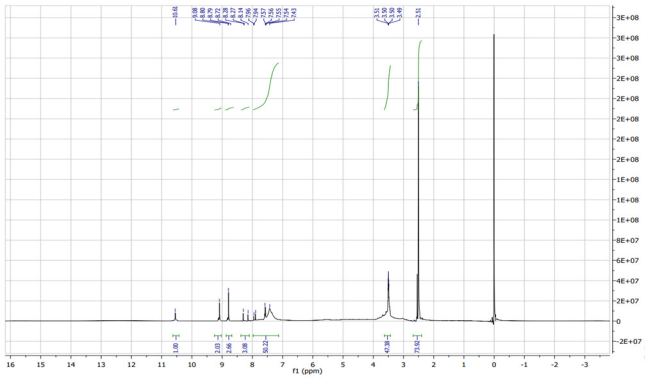

Fig. 11. ^{1}H-NMR spectrum for H_3 compound

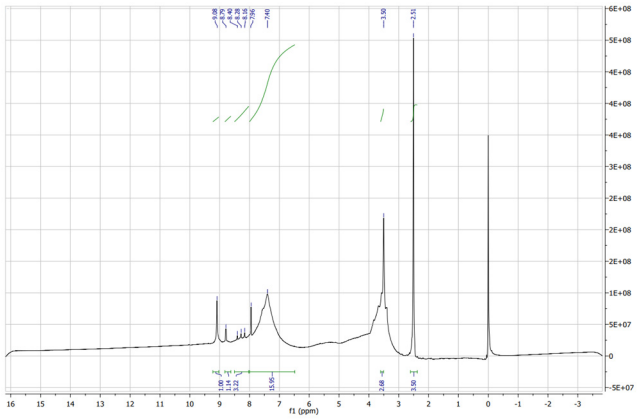

Fig. 12. ^{1}H-NMR spectrum for H_4 compound

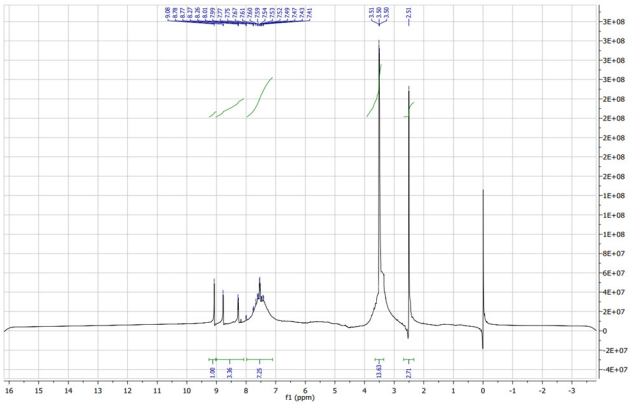

Fig. 13. ^{1}H-NMR spectrum for H_5 compound

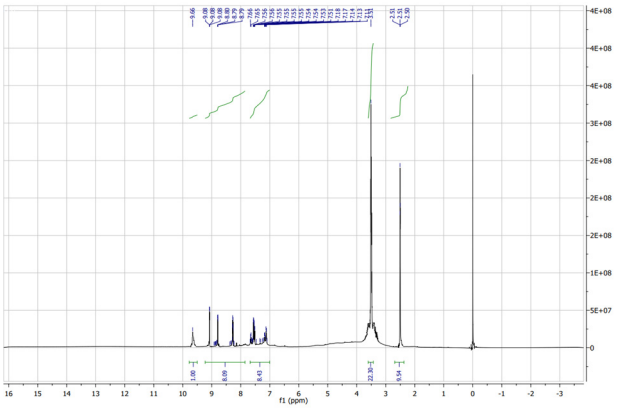

Fig. 14. ^{1}H-NMR spectrum for H_6 compound

3.3. Mass spectrum. All GC–MS chromatograms of the synthesized products exhibited a single peak with retention times ranging from 0.90 to 0.94 min, indicating the high purity of the newly prepared compounds [44, 45]. The corresponding mass spectra display plots of relative abundance versus *m/z*, with intense and characteristic peaks observed for all compounds, confirming that the fragmentation patterns are consistent with the proposed molecular structures. The GC–MS chromatograms and mass spectra are presented below (Fig.s 15-20), while detailed fragmentation analyses are summarized in Tables 4–9.

Table 4. Molecular fragmentations of H_1 compound

Fragments	Mass fragment to Charge formed (m / z)
$M^{\bullet+}$: $C_{41}H_{26}N_6O_{10}$	762.69
$C_{37}H_{26}N_5O_9^{\bullet+}$	683.22
$C_{34}H_{23}N_5O_7^{\bullet+}$	614.8
$C_{30}H_{27}N_4O_6^{+}$	540.56

$C_{25}H_{21}N_3O_5^+$	443.15
$C_{20}H_{19}N_3O_5^+$	381.01
$C_{18}H_{14}N_3O_5^+$	352.99
$C_{19}H_{13}N_2O_3^{\bullet+}$	316.07
$C_{16}H_{20}N_2O_3^{\bullet+}$	288.05
$C_{15}H_{18}N_2O_3^+$	Base peak 274.05
$C_{12}H_{10}N_2O_3^+$	230.05
$C_{10}H_5N_2O_3^{\bullet+}$	201.96
$C_8H_6NO_2^{\bullet+}$	148.04
$C_7H_9NO^+$	123.95
$^+C_5H_5N$	79.05

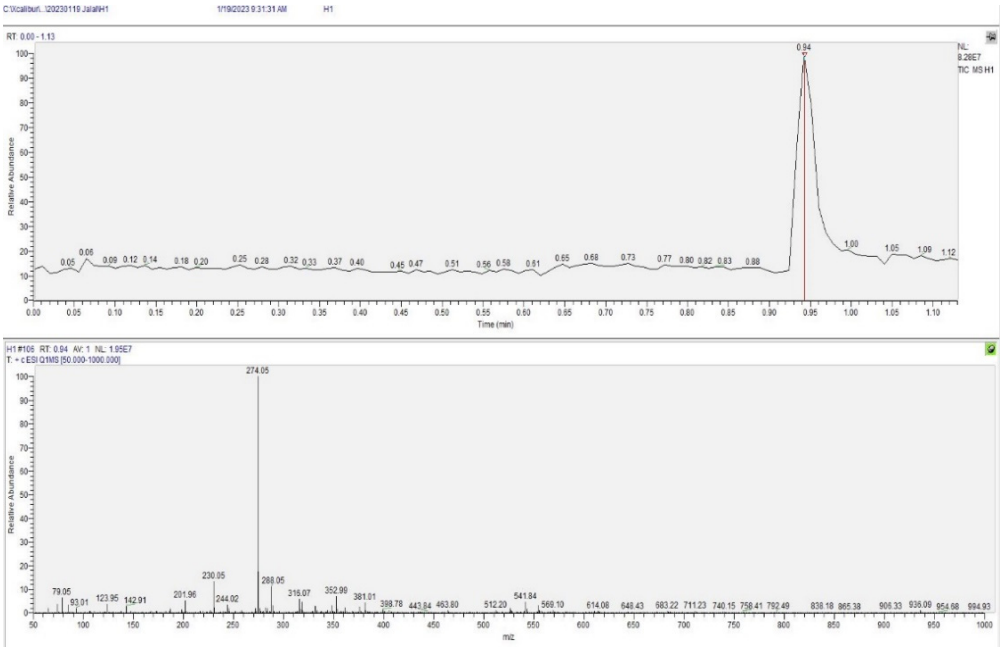

Fig. 15. GC-MS and Mass spectra of H_1 compound

Table 5. Molecular fragmentations of H_2 compound

Fragments	Mass fragment to Charge formed (m / z)
$M^{\bullet+}$: $C_{41}H_{26}Cl_2N_4O_6$	741.58
$C_{38}H_{23}Cl_2N_4O_4^{\bullet+}$	702.79
$C_{38}H_{30}Cl_2N_3O_4^{\bullet+}$	662.85
$C_{32}H_{26}Cl_2N_2O_3^+$	558.78
$C_{31}H_{26}Cl_2N_3O_4^+$	540.88
$C_{28}H_{23}ClN_3O_4^+$	500.89
$C_{25}H_{20}ClN_2O_3^+$	431.96
$C_{21}H_{15}Cl\ N_2O_3^{\bullet+}$	378.83
$C_{19}H_{14}ClN_2O_3^{\bullet+}$	352.95
$C_{19}H_{14}N_2O_3^{\bullet+}$	318.02
$C_{16}H_{18}N_2O_3^+$	287.99
$C_{15}H_{18}N_2O_3^+$	Base peak 274.04
$C_{14}H_{14}N_2O_3^{\bullet+}$	258.89
$C_{12}H_{10}N_2O_3^+$	230.03
$C_{13}H_{14}N_2^+$	198.95
$C_8H_8N_2O_3^+$	180.09
$C_5H_5N^+$	79.02
$C_4H_4N^+$	65.14

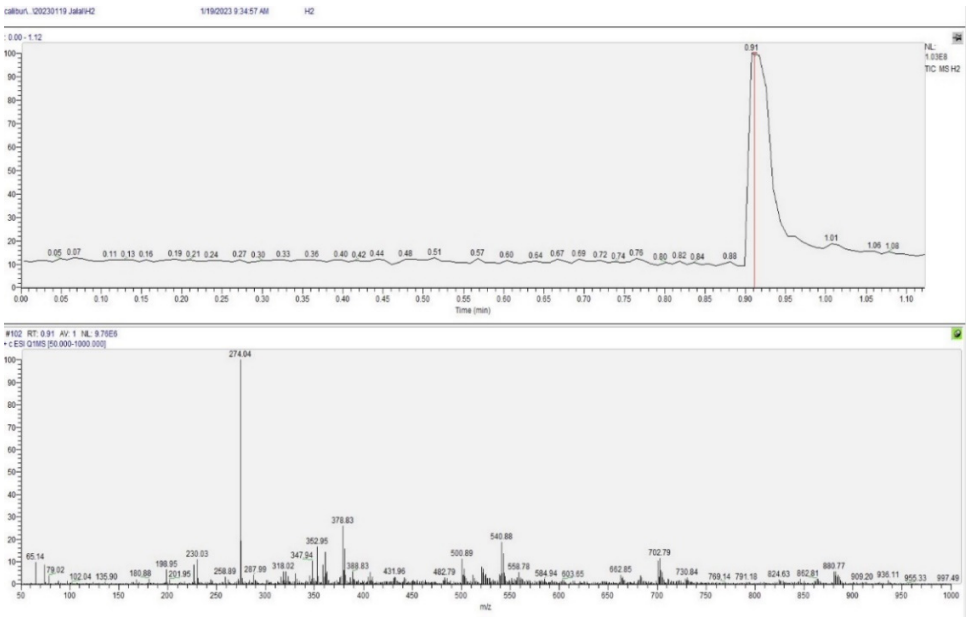

Fig. 16. GC-MS and Mass spectra of H_2 compound

Table 6. Molecular fragmentations of H_3 compound

Fragments	Mass fragment to Charge formed (m / z)
$M^{\bullet+} = C_{30}H_{17}Cl_2N_7O_6$	642.06
$C_{27}H_{17}Cl_2N_7O_6^+$	606.96
$C_{26}H_{19}Cl_2N_6O_6^+$	582.35
$C_{25}H_{20}Cl_2N_6O_5^+$	554.23
$C_{19}H_{19}ClN_6O_4^+$	431.82
$C_{17}H_{10}ClN_6O_3^{\bullet+}$	380.99
$C_{16}H_8ClN_5O_3^{\bullet+}$	352.99
$C_{15}H_{11}ClN_3O_3^{\bullet+}$	316.05
$C_{14}H_9ClN_2O_3^+$	288.04
$C_{14}H_9ClNO_3^+$	Base peak 274.04
$C_{12}H_{10}N_2O_3^+$	230.02
$C_{10}H_5N_2O_3^{\bullet+}$	201.97
$C_7H_9NO^+$	123.91
$C_5H_5N^+$	79.05
$C_4H_4N^+$	65.14

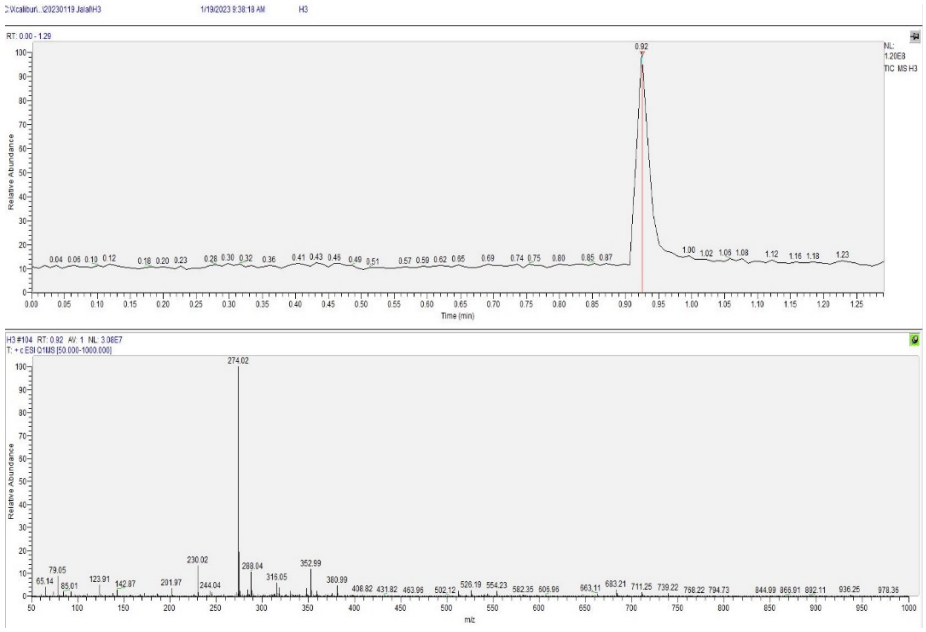

Fig. 17. GC-MS and Mass spectra of H_3 compound

Table 7. Molecular fragmentations of H_4 compound.

Fragments	Mass fragment to Charge formed (m / z)
$M^{\bullet+}$ =$C_{33}H_{19}Cl_2N_5O_6$	651.07
$C_{32}H_{25}Cl_2N_5O_4^+$	614.10
$C_{28}H_{23}Cl_2N_4O_6^+$	582.19
$C_{27}H_{23}Cl_2N_4O_5^+$	554.13
$C_{26}H_{22}Cl_2N_4O_4^+$	526.02
$C_{23}H_{23}ClN_4O_4^+$	455.70
$C_{19}H_{13}ClN_4O_3^{\bullet+}$	380.98
$C_{18}H_{11}ClN_3O_3^{\bullet+}$	352.96
$C_{17}H_{17}ClN_3O_3^+$	348.01
$C_{15}H_{11}ClN_3O_3^+$	316.06
$C_{14}H_9ClN_2O_3^+$	288.02
$C_{14}H_9ClNO_3^{\bullet+}$	Base peak 274.04
$^+C_{12}H_{10}N_2O_3$	230.04
$C_{10}H_5N_2O_3^{\bullet+}$	201.94
$C_9H_{10}N_2O^+$	162.92
$C_5H_5N^+$	79.05
$C_4H_4N^+$	65.13

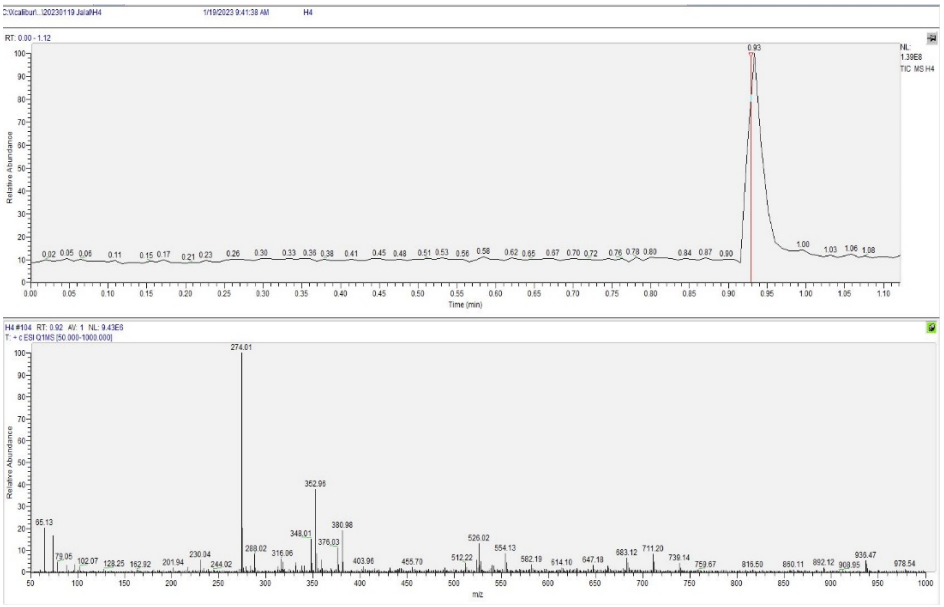

Fig. 18. GC-MS and Mass spectra of H_4 compound

Table 8. Molecular fragmentations of H_5 compound

Fragments	Mass fragment to Charge formed (m / z)
$M^{\bullet+}$ = $C_{33}H_{17}Cl_4N_5O_6$	721.56
$C_{31}H_{16}Cl_4N_4O_6^+$	681.77
$C_{29}H_{21}Cl_3N_4O_4^+$	595.68
$C_{27}H_{19}Cl_3N_4O_3^+$	554.22
$C_{27}H_{24}Cl_3N_4O^+$	526.18
$C_{21}H_{21}Cl_3N_3O^+$	437.79
$C_{18}H_{13}Cl_2N_3O_3^+$	390.78
$C_{15}H_{12}Cl_2N_3O_3^{\bullet+}$	352.94
$C_{16}H_{13}ClN_2O_3^+$	316.02
$C_{14}H_9ClN_2O_3^+$	288.02
$C_{14}H_9ClNO_3^{\bullet+}$	Base peak 274.04
$C_{12}H_9N_2O_3^{\bullet+}$	299.98
$C_8H_9N_2O_3^+$	181.91
$C_6H_7N_2O^{\bullet+}$	123.91
$C_5H_5N^+$	79.07
$C_4H_4N^+$	65.12

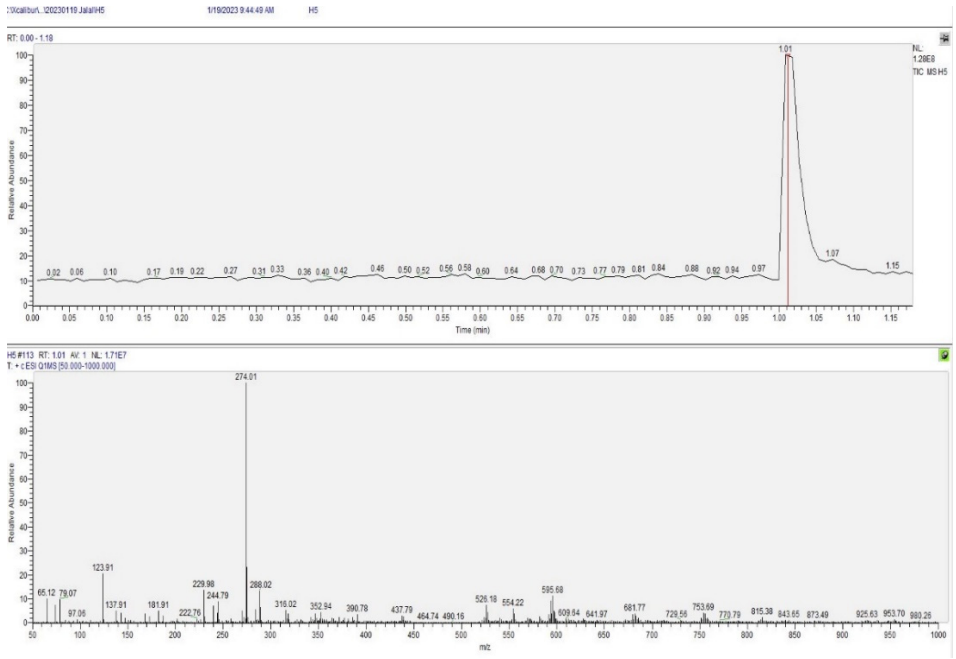

Fig. 19. GC-MS and Mass spectra of H_5 compound

Table 9. Molecular fragmentations of H_6 compound

Fragments	Mass fragment to Charge formed (m / z)
$M^{\bullet+} = C_{34}H_{22}N_4O_8$	614.57
$C_{33}H_{22}N_3O_8^{\bullet+}$	588.14
$C_{30}H_{24}N_3O_8^{+}$	554.15
$C_{25}H_{21}N_3O_5^{\bullet+}$	443.86
$C_{24}H_{17}N_3O_3^{+}$	426.86
$C_{20}H_{14}N_2O_4^{+}$	346.78
$C_{18}H_{20}N_2O_3^{+}$	312.15
$C_{17}H_{20}N_2O_2^{+}$	284.15
$C_{15}H_{17}N_2O_3^{\bullet+}$	Base peak 274.04
$C_{13}H_{14}N_2O_2^{+}$	230.11
$C_{12}H_{11}N_2O_2^{+}$	215.08
$C_9H_{11}NO_2^{+}$	165.08
$C_7H_9NO^{+}$	123.07
$C_6H_4^{+}$	75.04
$C_4H_4N^{+}$	65.12

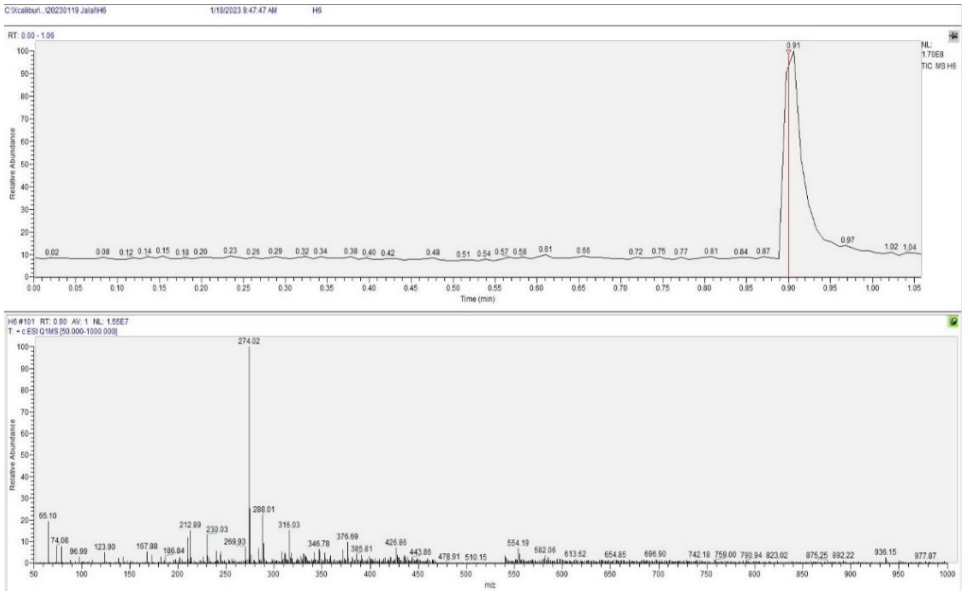

Fig. 20. GC-MS and Mass spectra of H_6 compound

3.4. Antioxidant activity of the new oxazepine derivatives compounds (H_1-H_6). The activity of the compounds was indicated by a color change of the reagent from purple to yellow, with a more intense yellow coloration signifying higher efficiency. Compounds H_1, H_4, and H_6 exhibited stronger antioxidant activity than vitamin C [46], indicating their superior potential as antioxidant agents. The present results show the free-radical scavenging activity of the efficiency compounds compared to vitamin C. The results in table 10 confirm the H_6 compound has the best capability of free-radical hunting.

Table 10. Activity of H_1, H_2, and H_6 compounds as anti-oxidant

Concentration (Mm)	Percentage of antioxidant activity (%)			
	H_1	H_4	H_6	Standard (Vitamin C)
0.05	21.8	14.8	37.4	63
0.1	23	17.5	44.3	65.7
0.15	26.7	22.6	51	69
0.2	34	29.4	57.6	76.8
0.5	41.3	32	66.5	87.6

$$\% \text{ Antiradical activity} = \frac{A_{\text{Control}} - A_{\text{Test}}}{A_{\text{Control}}} * 100$$

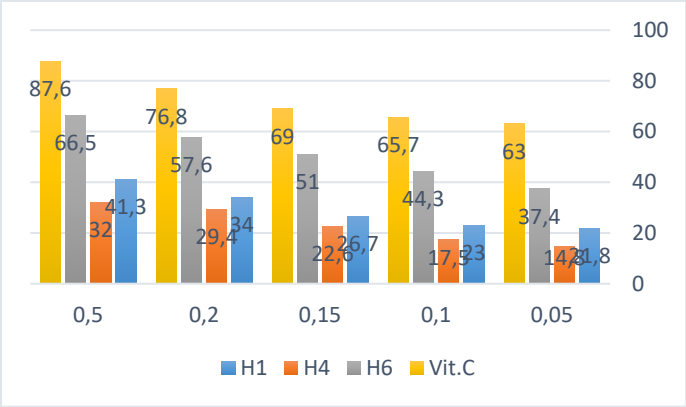

Fig. 21. Antioxidant activity of the H_1 H_4, and H_6 compounds

The IC_{50} for each compound were particular and display in the Table 11 and Fig.s 22 and 23.

Table 11. IC_{50} values of antioxidant activity of H_1, H_4 and H_6 compounds [48].

Compound	IC50 Mm
H_1	0.4600
H_4	0.5800
H_6	0.2700
Vitamin C	0.2049

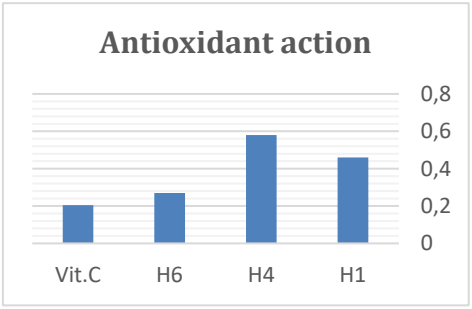

Fig. 22. IC_{50} antioxidant activity of H_1, H_4 and H_6 compounds (the statistics were performed using Microsoft Excel)

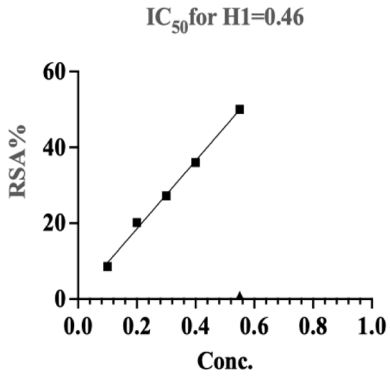

Fig. 23. The IC_{50} for H_1 (the graph was performed using Prism Graph Pad software 9.0)

3.5. The molecular docking and computational simulation of the new oxazepine derivatives compounds (H_1-H_6) as antioxidant agents. In order to determine the optimal binding locations and the length of the bonds to neighboring residues in the protein, molecular docking of H_1, H_4, and H_6 with Tyrosinase (PDB ID: 3NM8) was performed [33]. With the Tyrosinase enzyme, several binding sites displayed varying binding energies. Nonetheless, the Tyrosinase enzyme with the lowest binding energy among the produced compounds was chosen for more examination and visualization. Molecular docking of H_1, H_4, and H_6 with Tyrosinase (PDB ID: 3NM8) was performed to find the best binding sites and the length of the bonds to nearby residues in the protein [33]. A number of binding sites showed different binding energies with the Tyrosinase enzyme. However, out of all the compounds that were created, the Tyrosinase enzyme with the lowest binding energy was selected for further analysis and visualization, as stated in the previous studies [13, 14].

The docking results for H_1 with Tyrosinase (PDB ID: 3NM8) showed six hydrogen bonds with the following residues: Arg 6A, Arg 75A, Arg 75A, Arg 78A, Arg 78A, and Asn 270B. However, π cation interactions were shown with Arg 78A. Also, the H_1 compound showed a reasonable binding affinity with approximately −6.4 kcal/mol with Tyrosinase.

The docking results for H4 with Tyrosinase (PDB ID: 3NM8) showed only two hydrogen bonds with the following residues: Thr 137B and Phe 258A. However, three hydrophobic interactions were found to bind to the prepared compounds with bond lengths less than 3.5 angstroms with Tyrosinase enzyme at Pro 51A, Thr 137B, and Phe 258A. Also, the H_4 compound showed a reasonable binding affinity with approximately −6.7 kcal/mol with Tyrosinase.

On the other hand, the docking results for compound H_6 with tyrosinase (PDB ID: 3NM8) revealed the formation of only two hydrogen bonds involving residues Asp55A and Asn57A. However, three hydrophobic interactions were shown with bond lengths less than 3.5 angstroms with Tyrosinase enzyme at Pro 201A and Val 218A at two sites. Also, H_4 compound showed a reasonable binding affinity with approximately −6.7 kcal/mol with Tyrosinase. However, π cation interactions were shown with Arg 209A and also a salt bridge at Arg 209˚A. All selected docked proteins with prepared compounds H_1, H_4, and H_6 have shown RMSD scores of 1.16, 1.4, and 1.3, respectively. H_4 compound has also shown the best binding affinity, fairly similar to the experimental assessment. Collectively, it can be clearly seen that the prepared compounds have shown fair antioxidant activity, which needs further in vivo investigations.

Table 12. Selected specific interactions between protein residues and the prepared compounds, with bond lengths measured in angstroms (Å)

PDB	Specific interactions	Residue	Amino acid	Distance H-A
H_1	Hydrogen Bond	6A	Arg	2.8
		75A	Arg	2.8
		75A	Arg	2.2
		78A	Arg	2.8
		78A	Arg	2.0

		270B	Asn	3.0
	π-stacking	78A	Arg	3.0
H4	Hydrophobic Interaction	51A	Pro	3.4
		137B	Thr	3.4
		258A	Phe	3.8
	Hydrogen Bond	137B	Thr	2.2
		258A	Phe	2.5
H6	Hydrophobic Interaction	210A	Pro	3.8
		218A	Val	3.6
		218A	Val	3.6
	Hydrogen Bond	55A	Asp	2.1
		57A	Asn	2.1
	π-stacking	209A	Arg	4.2
	Salt bridge	209A	Arg	5.0

In silico molecular docking and simulation methods are widely used in pharmaceutical research, particularly in combination with artificial intelligence techniques [47–54]. Typically, the binding affinity of newly synthesized biomolecules toward target proteins is evaluated through computational simulations prior to experimental investigation [13].

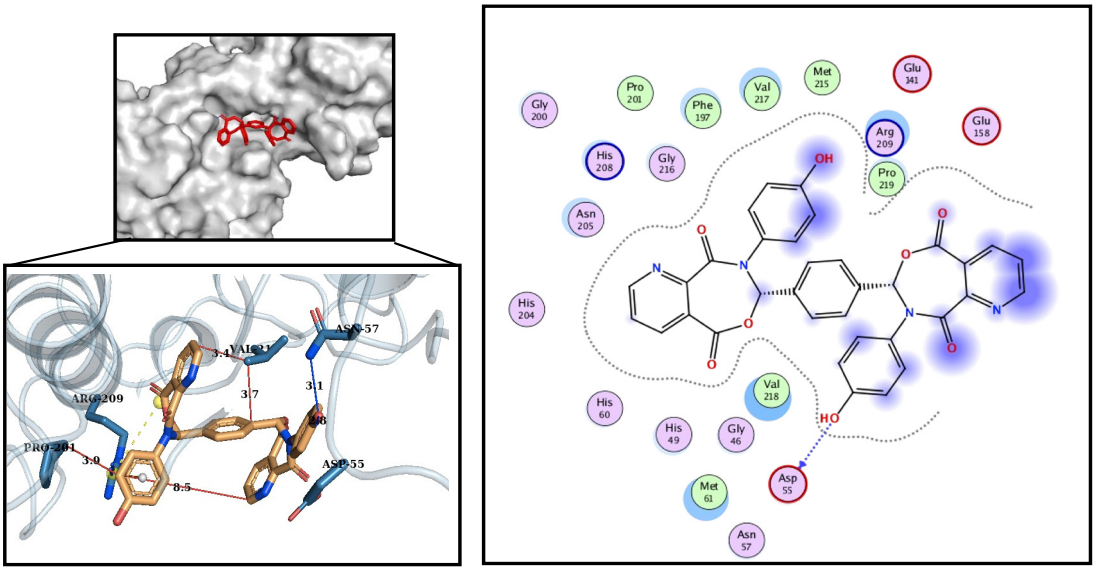

Fig. 24. Molecular docking representation of the synthesized compound H1 (shown in red and orange) bound to tyrosinase (reductase enzyme, PDB ID: 3NM8), displayed in grey. The docking pose was visualized using PyMOL based on the MOE-generated PDB file

In this study, the binding affinity of novel homo-oxazepine dimer derivatives, designated H1, H4, and H6, toward the reductase enzyme (PDB ID: 3NM8) was investigated using molecular docking in order to evaluate their antioxidant potential (Fig.s 23-26). Consistent with the docking results, experimental antioxidant assays revealed that compound H4 exhibited the highest antioxidant activity. Compound H1 showed lower activity than both H4 and H6 and displayed the weakest antioxidant performance among the studied derivatives. Nevertheless, all prepared compounds demonstrated superior antioxidant activity compared with the control (vitamin C). Docking analysis indicated that compound H4 formed two hydrogen bonds with residues Thr137B and Thr258A, with favorable bond lengths of approximately 2.0 Å. In addition, three hydrophobic interactions involving Pro51A, Thr137B, and Thr258A were observed, which may contribute to the enhanced binding affinity of this compound. In contrast, compound H1 formed six hydrogen bonds and only one π–π stacking interaction, a binding mode that may account for its lower affinity relative to H4. Compound H6 exhibited intermediate antioxidant activity, which can be attributed to the formation of two hydrogen bonds with Asp55A and Asp57A, along with three relatively weaker hydrophobic interactions (~3.0

Å), π–π stacking interactions with Arg209A, and a salt bridge at the same residue with a bond length of approximately 5.0 Å.

Overall, the experimental antioxidant activities showed good agreement with the *in silico* docking results. These findings clearly indicate that variations in binding-site geometry and functional group interactions significantly influence the biological activity of homo-oxazepine dimers [35].

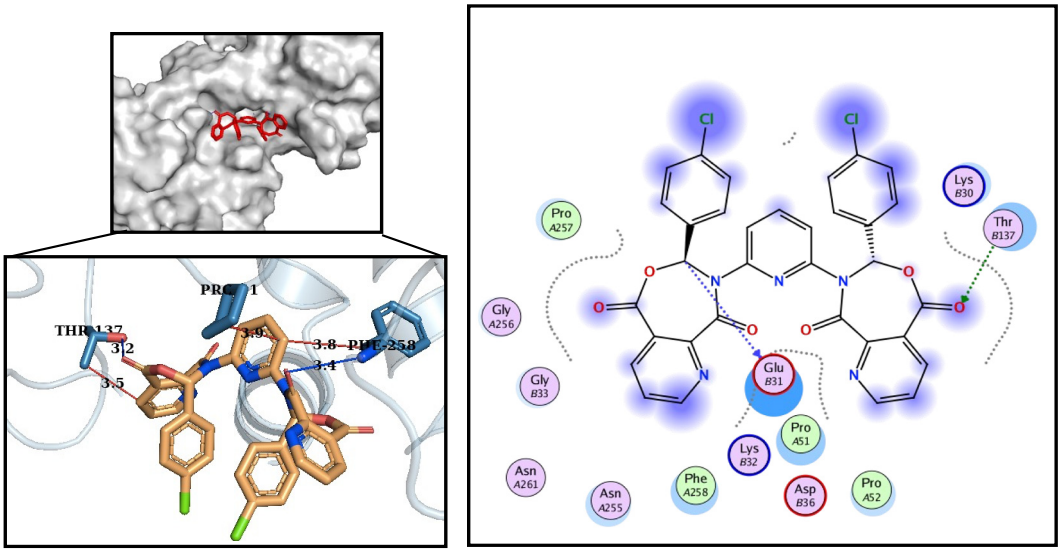

Fig. 25. Molecular docking representation of the synthesized compound H_4 (shown in red and orange) bound to tyrosinase (reductase enzyme, PDB ID: 3NM8), displayed in grey. The docking pose was visualized using PyMOL based on the MOE-generated PDB file

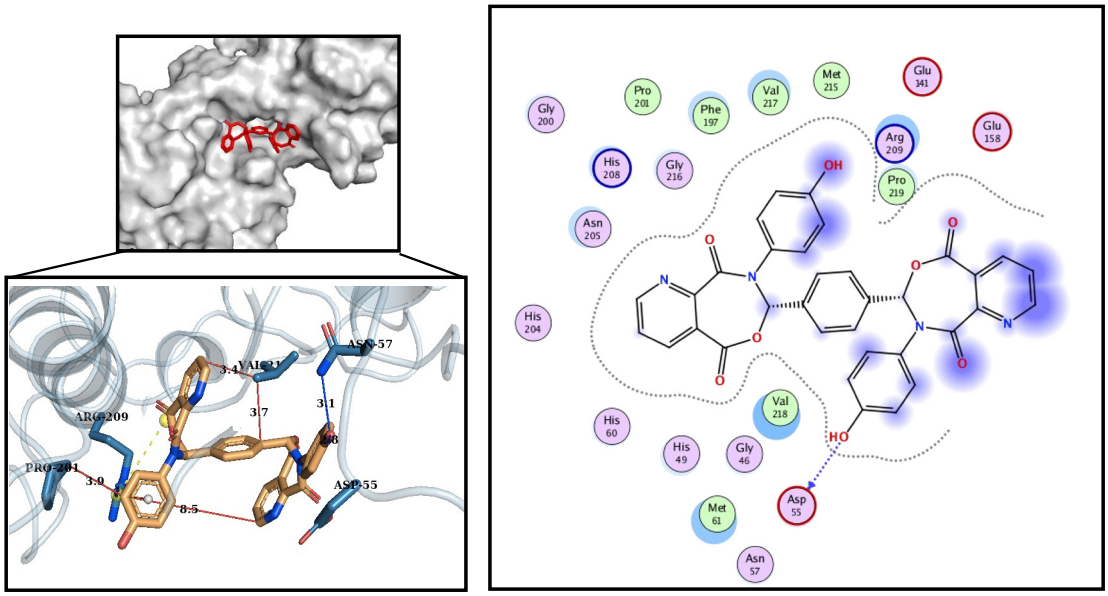

Fig. 26. Molecular docking representation of the synthesized compound H_6 (shown in red and orange) bound to tyrosinase (reductase enzyme, PDB ID: 3NM8), displayed in grey. The docking pose was visualized using PyMOL based on the MOE-generated PDB file

Conclusion

The aim of this study was to synthesize a series of oxazepine derivatives via the condensation of amines with various benzaldehyde derivatives using benzene as the solvent. The resulting intermediates were subsequently reacted with pyridine-5,7-dione anhydride in dry benzene to afford oxazepine derivatives (H_1–H_6). The synthesized compounds were structurally characterized by Fourier-transform infrared spectroscopy (FT-IR), proton nuclear magnetic resonance (^{1}H-NMR)

spectroscopy, and mass spectrometry, confirming the successful formation of the target structures. Reaction progress at each stage was monitored by thin-layer chromatography (TLC).

The antioxidant activity of compounds H_1–H_6 was evaluated in comparison with vitamin C, and all synthesized derivatives exhibited superior antioxidant performance relative to the control. In addition, molecular docking studies of selected compounds (H_1, H_4, and H_6) with tyrosinase (PDB ID: 3NM8) were conducted to identify optimal binding modes and interactions with neighboring amino acid residues. The docked complexes showed RMSD values of 1.16, 1.40, and 1.30 for H_1, H_4, and H_6, respectively, indicating reliable docking poses. Among the studied compounds, H_4 demonstrated the most favorable binding affinity, in good agreement with the experimental antioxidant results.

Overall, the combined experimental and *in silico* findings suggest that the synthesized oxazepine derivatives possess promising antioxidant activity. Nevertheless, further *in vivo* investigations are required to fully assess their biological potential.

Acknowledgments

The co-authors of the research would like to acknowledge the support and contribution of the University of Anbar (www.uoanbar.edu.iq) through all their distinguished and distinguished academic staff in encouraging and supporting this new research with all the required technical, scientific, academic and research support.

References

1. Abbas A.K., Jber N.R. Synthesis and estimation of biological activity of new oxazepine derivatives. *Int J Pharm Res*. 2020, **Vol. 12(2)**, p. 3750–3758. DOI: 10.31838/ijpr/2020.SP2.457
2. Muhammad F.M., Khairallah B.A., Albadrany K.A. Synthesis, characterization and antibacterial evaluation of novel 1, 3-oxazepine derivatives using a cycloaddition approach. *J Angiother.* 2024, **Vol. 8(3)**, p. 1–5. DOI: 10.25163/angiotherapy.839506
3. Hamak K.F., Eissa H.H. Synthesis, characterization, biological evaluation and anti corrosion activity of some heterocyclic compounds oxazepine derivatives from Schiff bases. *Org Chem Curr Res*. 2013, **Vol. 2(3)**, 1000121. DOI: 10.4172/2161-0401.1000121
4. Aftan M.M., Jabbar M.Q., Dalaf A.H., Salih H.K. Application of biological activity of oxazepine and 2-azetidinone compounds and study of their liquid crystalline behavior. *Mater Today Proc*. 2021, **Vol. 43(2)**, p. 2040–2050. DOI: 10.1016/j.matpr.2020.11.838
5. Sahap E.H., Adam R.W., Razzaq Z.L. Synthesis and Characterization of Some New 1, 3-Oxazepine and 1, 3-Diazepine Derivatives Combined with Azetidine-2-one. *Journal of Global Pharma Technology*, 2018, **Vol. 10 (03),** p. 289-297
6. Hassan A.S., Hame A.S. Study of antimicrobial activity of new prepared seven membered rings (Oxazepine). *Res J Biotechnol*. 2019, **Vol. 14(Special Issue 1)**, p. 109–118.
7. Mamouni A., Daïch A., Marchalin S., Decroix B. Azepine and [1, 3] oxazepine fused ring construction through a cationic cyclization: An N-acyliminium ion trapping of an oxygen atom or olefin. *Heterocycles*, 2001. **Vol. 54(1)**, p. 275–282.
8. Faisca Phillips A.M.M.M., Pombeiro A.J.L. *Modern Methods for the Synthesis of 1, 4-Oxazepanes and Their Benzo-Derivatives*. *Synth Approaches to Nonaromatic Nitrogen Heterocycles*. 2020. Chapter 15. p. 437–500. DOI: 10.1002/9781119708841.ch15#
9. Noser A.A., El-Barbary A.A., Salem M.M., El Salam H.A.A., Shahien M. Synthesis and molecular docking simulations of novel azepines based on quinazolinone moiety as prospective antimicrobial and antitumor hedgehog signaling inhibitors. *Sci. Rep.* 2024, **Vol. 14(1)**, 3530. DOI: 10.1038/s41598-024-53517-y
10. Al-Khuzaie M.G., Al-Majidi S.M. Synthesis and characterization of some new benzothiazine, dihydroquinazolinone and oxazepine derivatives from 1, 8-naphthalic anhydride and evaluation of their antimicrobial activity. *J Glob Pharma Technol*. 2018, **Vol. 10(11)**, p. 415–423.
11. Thummala Y., Raju C.E., Purnachandar D., Sreenivasulu G., Doddi V.R., Karunakar G.V. Gold-

Catalyzed Regioselective Synthesis of Pyrazolo [1, 4] oxazepines via Intramolecular 7-endo-dig Cyclization. *European J Org Chem*. 2020, **Vol. 2020(24)**, p. 3560–3567. DOI: 10.1002/ejoc.201901852

12. Jaffer N.D. Synthesis, Characterization, and Evaluation of Antioxidant and Physical Properties of New Bifunctional Aromatic Monomers Containing Imine and Heterocyclic Rings in The Main Chain. J Kufa Chem Sci. 2023, Vol. 3(1), p. 395–414. DOI: 10.36329/jkcm/2023/v3.i1.13855
13. Farhan M.M., Guma M.A., Rabeea M.A., Ahmad I., Patel H. Synthesizes, characterization, molecular docking and in vitro bioactivity study of new compounds containing triple beta lactam rings. *J Mol Struct*. 2022, **Vol. 1269**, 133781. DOI:10.1016/j.molstruc.2022.133781
14. Jabbar A.S., Guma M.A., Muslim R.F. Preparation, spectral characterization, in silico ADME studies, molecular docking, and antioxidant activity of some derivatives of the Oxazepine symmetrical dimers. *AIP Conference Proceedings*, 2025, 3303, 040009. DOI: 10.1063/5.0264112
15. Martins D.A., Bomfim Filho L.F., da Silva C.M., de Fátima Â., Louro S.R.W., Batista D.G.J., Soeiro M.N.C., de Carvalho J.E., Teixeira L.R. Copper (II) nitroaromatic Schiff base complexes: synthesis, biological activity and their interaction with DNA and albumins. *J Braz Chem Soc*. 2017, **Vol. 28(1)**, p. 87–97. DOI: 10.5935/0103-5053.20160150
16. Almashal F.A., Mohammed M.Q., Hassan Q.M.A., Emshary C.A., Sultan H.A., Dhumad A.M. Spectroscopic and thermal nonlinearity study of a Schiff base compound. *Opt Mater (Amst)*, 2020, **Vol. 100**, 109703. DOI: 10.1016/j.optmat.2020.109703
17. Wang Y., Jin Z., Zhou L., Lv X. Recent advances in [4+ 4] annulation of conjugated heterodienes with 1, 4-dipolar species for the synthesis of eight-membered heterocycles. *Org Biomol Chem*, 2024, **Vol. 22(2)**, p. 252–268. DOI: 10.1039/D3OB01626A
18. Jaber Q.A.H., Shentaif A.H., Almajidi M., Ahmad I., Patel H., Azad A.K., Alnasser S.M., Alatawi H.A., Menaa F., Alfaifi S.Y.M., Rahman M.M., Ali M.M., Aditya Rao S.J. Synthesis, structure, and in vitro pharmacological evaluation of some new pyrimidine-2-sulfonamide derivatives and their molecular docking studies on human estrogen receptor alpha and CDK2/Cyclin proteins. *Russ J Bioorganic Chem*. 2023, **Vol. 49(Suppl 1)**, S106–118. DOI: 10.1134/S1068162023080095
19. de Fátima Â., de Paula Pereira C., Olímpio C.R.S.D.G., de Freitas Oliveira B.G., Franco L.L., da Silva P.H.C. Schiff bases and their metal complexes as urease inhibitors–a brief review. *J Adv Res.* 2018, Vol. 13, p. 113–126. DOI: 10.1016/j.jare.2018.03.007
20. Abdulridha M.M., Hassan B.A., Baqer F.M. Design, characterisation, molecular docking, and cytotoxicity study of new 5-phenyl-4h-1, 2, 4-triazole-3-thiol schiff bases derivatives. *Chemical Problems*, 2026, in press
21. Hassan B.A., Hamed F.M. Synthesis and pharmaceutical Activity of triazole Schiff Bases with theoretical Characterization. *Chemical Problems,* 2024, **Vol. 22(3)**, p. 332–341. DOI: 10.32737/2221-8688-2024-3-332-341
22. Zhang Y., Wang C., Jia Z., Ma R.J., Wang X.F., Chen W.Y., Liu K.-Ch. Isoniazid promotes the anti-inflammatory response in zebrafish associated with regulation of the PPARγ/NF-κB/AP-1 pathway. *Chem Biol Interact*, 2020, **Vol. 316**, 108928. DOI: 10.1016/j.cbi.2019.108928
23. Muslim R.F., Majeed I.Y., Saleh S.E., Saleh M.M., Owaid M.N., Abbas J.A. Preparation, Characterization and Antibacterial Activity of some New Oxazolidin-5-one Derivatives Derived from Imine Compounds. *J Chem Heal Risks*. 2022, Vol. 12(4), p. 725-732.
24. Hamil A., Khalifa K.M., Almutaleb A.A., Nouradean M.Q. Synthesis, characterization and antibacterial activity studies of some transition metal chelates of Mn (II), Ni (II) and Cu (II) with Schiff base derived from diacetylmonoxime with O-phenylenediamine. *Adv J Chem A*. 2020, **Vol. 3(4)**, p. 524–533. DOI: 10.33945/SAMI/AJCA.2020.4.13
25. Tawfeeq H.M., Muslim R.F., Abid O.H., Owaid M.N. Synthesis and characterization of novel tetrazole derivatives and evaluation of their anti-candidal activity. *ACTA Pharm Sci.* 2019, **Vol. 57(3),** p. 45-63. DOI: 10.23893/1307-2080.APS.05717
26. Saleh A., Saleh M.Y. Synthesis of heterocyclic compounds by cyclization of Schiff bases

prepared from capric acid hydrazide and study of biological activity. *Egypt J Chem*. 2022, **Vol. 65(12)**, p. 783–92. DOI: 10.21608/ejchem.2022.133946.5904
27. Abdulkarim A.Z., Sani U., Adamu S.L. Synthesis, Characterization, Cytotoxicity and Antimicrobial Studies of Schiff Base Derived From 2-Benzoylbenzoic acid and 4-Nitro aniline and Its Metal (II) Complexes. *FUDMA J Sci*. 2023, **Vol. 7(6)**, p. 200–205. DOI: 10.33003/fjs-2023-0706-2104
28. Ay E. Synthesis and characterization of Schiff base 1-Amino-4-methylpiperazine derivatives. *Celal Bayar Univ J Sci*. 2016, **Vol. 12(3)**, p. 375–392. DOI: 10.18466/cbayarfbe.280600
29. Tawfeeq H.M., Muslim R.F., Abid O.H., Owaid M.N. Synthesis and characterization of novel five-membered heterocycles and their activity against Candida yeasts. *Acta Chim Slov*. 2019, **Vol. 66(3)**, p. 552–559.

Kshash A.H. Synthesis and characterization of tetrachloro-1, 3-oxazepine derivatives and evaluation of their biological activities. *Acta Chim Slov*. 2020, **Vol. 67(1)**, p. 113–118. DOI: 10.17344/acsi.2019.5264

31. Ayfan A.H., Muslim R.F., Saleh M.M. Preparation, Diagnoses of novel hetero atom compounds and Evaluation the Antibacterial Activity of them. *Res J Pharm Technol.* 2021, **Vol. 14(1)**, p. 79–84. DOI: 10.5958/0974-360X.2021.00015.9
32. Omar F.A., Hamad A.S., Taha N.I. Synthesis, Characterization and Evaluation Antibacterial Activity of Some (1, 3-Oxazepine-4, 7-dione and 1, 3-Benzooxazepine-4, 7-dione) Derived from Sulphamethoxazole using Irradiation Method. *Kirkuk Univ Journal-Scientific,* 2022, Vol. 17(2), p. 27-35. DOI: 10.32894/kujss.2022.131552.1048#
33. Sendovski M., Kanteev M., Ben-Yosef V.S., Adir N., Fishman A. First structures of an active bacterial tyrosinase reveal copper plasticity. *J Mol Biol*. 2011, **Vol. 405(1)**, p. 227–237. DOI: 10.1016/j.jmb.2010.10.048#
34. Fedorov D.G. The fragment molecular orbital method: theoretical development, implementation in GAMESS, and applications. *Wiley Interdiscip Rev Comput Mol Sci*., 2017, **Vol. 7(6)**, e1322. DOI: 10.1002/wcms.1322
35. Ibrahim K.K., Muslim R.F. Synthesis, characterisation, molecular docking and in vitro antioxidant and antifungal activity evaluation of new Thiazolidin-4-one derivatives. *AIP Conference Proceedings*, 2025, **Vol. 3303**, p. 070012. DOI: 10.1063/5.0264109
36. Cao Y., Li L. Improved protein–ligand binding affinity prediction by using a curvature-dependent surface-area model. *Bioinformatics*, 2014, **Vol. 30(12)**, p. 1674–1680. DOI: 10.1093/bioinformatics/btu104
37. Ahmed A.H., Muslim R.F., Abdullah I.Q., Abdulrazzaq Z.K. Characterization, antioxidant and biological activity of triphenyl-λ5–phosphaneylidene-1, 3-oxazepine-4, 7-dione compound synthesized from di-azomethine compounds. *AIP Conference Proceedings*, 2023, **Vol. 2834**, 030023. DOI:10.1063/5.0161499
38. Abid O.H., Tawfeeq H.M., Muslim R.F. Synthesis and Characterization of Novel 1, 3-oxazepin-5 (1H)-one Derivatives via Reaction of Imine Compounds with Isobenzofuran-1 (3H)-one. *ACTA Pharm Sci.* 2017, **Vol. 55(4)**, 104062287. DOI:10.23893/1307-2080.APS.05525
39. Aftan M.M., Talloh A.A., Dalaf A.H., Salih H.K. Impact para position on rho value and rate constant and study of liquid crystalline behavior of azo compounds. *Mater Today Proc.* 2021, **Vol. 45(6)**, p. 5529–5534. DOI: 10.1016/J.MATPR.2021.02.298
40. Berthomieu C., Hienerwadel R. Fourier transform infrared (FTIR) spectroscopy. *Photosynth Res.* 2009, **Vol. 01(2–3)**, p. 157–170. DOI:10.1007/s11120-009-9439-x
41. Mohamed M.A., Jaafar J., Ismail A.F., Othman M.H.D., Rahman M.A. Fourier Transform Infrared (FTIR) Spectroscopy. *Membrane Characterization*, 2017, p. 3–29. DOI:10.1016/B978-0-444-63776-5.00001-2
42. Muslim R.F., Guma M.A., Abedulrahman M.F., Ahmad I., Patel H., Rabeea M.A. Synthesizes, characterization, molecular modelling studies and bioactivity of a novel bicyclic compound of δ-lactam with oxazepine ring containing-sulphur substitute using an economic method. *Journal of*

Computational Biophysics and Chemistry, 2025, **Vol. 24(6)**, p. 733-750. DOI: 10.1142/S2737416524500807

43. Nadr R.B., Abdulrahman B.S. Synthesis and characterization of a new series of [1, 3]-oxazepine compounds from heterocyclic schiff bases. *Zanco J Pure Appl Sci*. 2023, **Vol. 35(2)**, p. 197–210. DOI: 10.21271/ZJPAS.35.2.21
44. Mohammed M.A., Al-Darwesh M.Y., Muslim R.F., Rabeea M.A. Synthesis, characterization and anti-tumor application of a novel Zinc (II)-L-ascorbic acid derivative (TJPS-2021-0344. R1). *Thai J Pharm Sci.* 2022, **Vol. 46(2)**, p. 127-136
45. Hafidh S.H., Muslim R.F., Awad M.A. Characterization and biological effectiveness of synthesized complexes of Palladium (II) from imine compounds. *Egypt J Chem*. 2022, **Vol. 65(1)**, p. 385–396. DOI: 10.21608/EJCHEM.2021.79085.3876
46. Aftan M.M., Toma M.A., Dalaf A.H., Abdullah E.Q., Salih H.K. Synthesis and characterization of new azo dyes based on thiazole and assess the biological and laser efficacy for them and study their dyeing application. *Egypt J Chem*. 2021, **Vol. 64(6)**, p. 2903–2911. DOI: 10.21608/EJCHEM.2021.55296.3163
47. Dias R., de Azevedo J., Walter F. Molecular docking algorithms. *Curr Drug Targets*. 2008, **Vol. 9(12)**, p. 1040–1047. DOI: 10.2174/138945008786949432
48. Fadahunsi A.A., Uzoeto H.O., Okoro N.O., Cosmas S., Durojaye O.A., Odiba A.S. Revolutionizing drug discovery: an AI-powered transformation of molecular docking. *Med Chem Res*. 2024, **Vol. 33(12)**, p. 2187–2203. DOI: 10.1007/s00044-024-03253-9
49. Gao W., Ma X., Yang H., Luan Y., Ai H. Molecular engineering and activity improvement of acetylcholinesterase inhibitors: Insights from 3D-QSAR, docking, and molecular dynamics simulation studies. *J Mol Graph Model*. 2022, **Vol. 116**, 108239. DOI: 10.1016/J.JMGM.2022.108239
50. Zhang J., Chen D., Xia Y., Huang Y.P., Lin X., Han X., Ni N., Wang Z., Yu F., Yang L., Yang Y.I., Gao Y.Q. Artificial intelligence enhanced molecular simulations. *J Chem Theory Comput*. 2023, **Vol. 19(14)**, p. 4338–5430. DOI: 10.1021/acs.jctc.3c00214
51. Fan J., Fu A., Zhang L. Progress in molecular docking. *Quant Biol.* 2019, **Vol. 7(2)**, p. 83–89. DOI: 10.1007/S40484-019-0172-y#
52. Meng X.Y., Zhang H.X., Mezei M., Cui M. Molecular docking: a powerful approach for structure-based drug discovery. *Curr Comput Aided Drug Des*. 2011, **Vol. 7(2)**, p. 146–157. DOI: 10.2174/157340911795677602
53. Santos L.H.S., Ferreira R.S., Caffarena E.R. Integrating molecular docking and molecular dynamics simulations. In: *Docking screens for drug discovery*. Springer; 2019. p. 13–34. DOI: 10.1007/978-1-4939-9752-7_2
54. Singh S., Baker Q.B., Singh D.B. Molecular docking and molecular dynamics simulation. In: *Bioinformatics*. Elsevier; 2022. p. 291–304.